

MEASUREMENT OF TURBULENT SKIN FRICTION DRAG COEFFICIENTS PRODUCED BY DISTRIBUTED SURFACE ROUGHNESS OF PRISTINE MARINE COATINGS

Frederik Zafiryadis, Knud Erik Meyer
Department of Mechanical Engineering
Technical University of Denmark
DK-2800 Kgs. Lyngby
frederik@zafiryadis.dk

F. Gökhan Ergin
Dantec Dynamics
DK-2740 Skovlunde
gen@dantecdynamics.com

ABSTRACT

Skin friction drag coefficients are determined for marine antifouling coatings in pristine condition by use of Constant Temperature Anemometry (CTA) with uni-directional hot-wires. Mean flow behaviour for varying surface roughness is analysed in zero pressure gradient, flat plate, turbulent boundary layers for Reynolds numbers from $Re_x = 1.91 \times 10^5$ to $Re_x = 9.54 \times 10^5$. The measurements were conducted at the Technical University of Denmark in a closed-loop wind tunnel redesigned for investigations as this. Ensemble averages of the boundary layer velocity profiles allowed for determination of skin friction drag coefficients as well as roughness Reynolds numbers for the various marine coatings across the range of Re_x by fitting of the van Driest profile. The results demonstrate sound agreement with the present ITTC method for determining skin friction coefficients for practically smooth surfaces at low Reynolds numbers compared to normal operation mode for the antifouling coatings. Thus, better estimates for skin friction of rough hulls can be realised using the proposed method to optimise preliminary vessel design.

INTRODUCTION

Drag on marine vessels consists of three fundamental parts: skin friction drag, pressure drag and residual drag. Each part contributes to the overall drag of the ship (Bixler & Bhushan, 2013). The size of the pressure drag is directly linked to the shape of the underwater hull. The skin friction drag, on the other hand, is caused by the streamwise shear stress on the hull surface exerted by the flow of the water, thus dependent on the morphology of the surface (Vorburger *et al.*, 1982). Lastly, residual drag accounts for the amount of energy responsible for the formation of bow- and stern waves. Chambers *et al.* (1978) proposed a method for determining each of these components, an empirical method which is still highly used today. Extensive effort has gone into developing ways of accurately determining and minimizing skin friction drag on marine vessels, since it can ac-

count for up to 90% of the total drag experienced by a ship in motion, even if the skin is free of biofouling (Schultz *et al.*, 2010). The accumulation of micro- and macroorganisms on the wetted surface of a ship hull causes an increase in surface roughness, frictional resistance, and fuel consumption as shown by Vorburger *et al.* (1982). To avoid settlement on ship hulls, coatings with antifouling properties, whether through biocides toxic to marine organisms or other technologies, are applied as a top coat on the wetted hull surface. The frictional resistance of the pristine coating is important as long as fouling with slime or barnacles remain absent, a period which increases as the coatings become more efficient. Since the ban of tributyl tin (TBT) in biocides in 2003 (Claire *et al.*, 2009) efforts to develop new and improved antifouling coatings within the legislation have been made. The state-of-the-art foul release coatings (FR) have shown most promising results by use of non-toxic silicone elastomers forming a self cleansing non-stick surface when subjected to fluid shear forces. Compared to traditional toxic based antifouling, FR coatings require a smooth surface finish. This has spurred an increase in frictional resistance prediction of antifouling coatings and effects of surface roughness on frictional resistance. These include studies by Grigson (1992), Schultz (2004), Yigit *et al.* (2014) and Benson (2005), presenting numerical as well as experimental ways of evaluating skin friction of rough plates. Candries *et al.* (2001) and Schultz (2004) further carried out experimental studies of the effect of fouling on drag using towing tank experiments to determine the resistance increase caused by the application of different paint systems. Despite the fairly large body of research that has been conducted on the subject, less attention has been given to acquiring accurate skin friction coefficients for different coatings across as span of hydraulically smooth and rough surfaces.

Based on the work of Ergin (2016) a measurement method is developed to allow for evaluation of equivalent sand grain roughness k_s of an antifouling coated surface, relating the drag increment of the surface to an equivalent

surface composed of uniform sand grains, as well as predicting skin friction coefficients to be applied in the ITTC-performance prediction method (Chambers *et al.*, 1978). This will allow for better skin friction estimates than traditional empirical relations do, and will provide the necessary quantification of novel antifouling hydrodynamic performance compared to traditional ones, needed for predictions in full-scale conditions.

The objective of the study is to develop a method for accurately determining skin friction drag coefficients of marine antifouling coatings to supersede the empirical relations used for smooth and rough surfaces in the ITTC method, thus allowing for improvements of modern ship design to be made. Numerical simulations to attain this goal are highly dependent on input parameters and boundary conditions in reference to the surface in question, without which the solution is inaccurate. Furthermore, when dealing with near wall flows numerical approaches are often simplified and inadequate. In this case proper experimental investigations allow for enlightenment in the matter. Using a hot-wire Constant Temperature Anemometry (CTA) measurement setup, it is feasible to evaluate the hydrodynamic performance of antifouling coatings used for ship hulls. By exposing a rough surface to an increasing range of flow speeds up to a point where the skin friction coefficient C_f becomes independent of the Reynolds number, $Re = U_0 x / \nu$, it is possible not only to make accurate predictions of the non-dimensional equivalent sand grain roughness k_s^+ and C_f , but also allow for extrapolation to full-scale applications. For general purposes the dimensionless group $k_s^+ = k_s u_\tau / \nu$ is used for non-dimensionalising the rough and smooth flow conditions, with $u_\tau = \sqrt{\tau_w / \rho}$ being the friction velocity, where τ_w is the wall shear stress and ρ is the density of the fluid. From knowledge of the roughness Reynolds number k_s^+ distinctions between a hydraulically smooth flow regime ($k_s^+ \leq 5$), a transitional regime ($5 \leq k_s^+ \leq 30 - 70$), and a fully rough flow regime for ($k_s^+ \geq 30 - 70$) can be made (van Driest, 1956).

EXPERIMENTAL FACILITIES AND METHODS

To achieve the objectives of the study, the 300 mm \times 300 mm \times 1800 mm test section of a closed-loop wind tunnel at the Technical University of Denmark was refitted by Ergin (2016) in order to perform automated boundary layer measurements. This allows for detailed insights in the effects of surface roughness on near wall flow behaviour. The design features include a sliding test section front window, computer-controlled traversing in three dimensions, angle of attack adjustment and zero-pressure-gradient alignment. The wind tunnel runs at a maximum speed of 40 m/s with a turbulence intensity of 0.15% – 0.2%, decreasing to 0.10% – 0.15% at an operating speed of 30 m/s and below. Boundary layer velocity measurements to evaluate different antifouling coatings for commercial use were performed on flat plates installed in streamwise direction in the test section of the wind tunnel.

The geometry of the plates are set forth by the dimensions of the test section allowing for the length of the plates to be 750 mm, with a height and thickness of 297 mm and 10 mm, respectively, thus preventing blockage effects. A rack for vertically mounting the plates was installed in the wind tunnel test section, placing the plates with a distance of 300 mm from the inlet to the leading edge. The inability of the scale-model testing to match the Reynolds of a

vessel in operation (e.g. $Re_L = 10^8 - 10^9$) to achieve full dynamic similarity, was initially overcome by attempting to reach a suitably high Reynolds number for the skin frictions to become practically constant. In total, four identical aluminium plates were constructed with a surface roughness of $R_a \approx 0.2 \mu\text{m}$ in order to limit the roughness of the plate itself, thus contaminating the results. Leading edges of the plates were rounded to minimize flow disturbance.

Coatings

In order to experimentally investigate the boundary layer response to changes in surface roughness due to various types of ship hull coatings, three of the four plates were coated with different antifouling coatings. Coatings were applied to the plates under ideal conditions and in agreement with relevant standards. The coatings have different structures, giving rise to varying surface finish and thus varying surface roughness when applied to the plates. The following pristine test surfaces were used:

Reference - non-coated aluminium surface serving as control surface.

SPC - plate coated with a traditional self polishing copolymer coating.

Epoxy - plate coated with an amine-adduct cured epoxy coating reinforced with glassflakes.

FR - plate coated with a silicone foul release coating containing no biocides.

The epoxy coating is not a traditional antifouling, but instead applied on ship decks to create a skidproof surface. It is included in the study to ensure distinctive difference in roughness of the surfaces. The test surfaces were numerically assessed prior to experiments using a stylus instrument with a 0.2 μm stylus tip. A 12.5 mm evaluation length was used with a short-wavelength 0.8 mm filter with a cut-off length of 2.5 mm, allowing for determination of roughness heights, with wavelengths above 0.8 mm being disregarded. Five sample profiles at different positions on the plate surfaces were taken to ensure proper results. The obtained parameters are listed in Table 1 and contains roughness parameters R_a , R_z , and $R_{z,max}$ along with the spacing parameter R_{Sm} . R_a is an arithmetic average taken over the 15 consecutive sampling lengths. R_z is an average of the peak-to-valley height from the 15 adjoining sample lengths, while the $R_{z,max}$ parameter determines the highest R_z related to the 15 sample lengths. Thorough definitions of the used parameters including relevant standards can be found in Whitehouse (1994) or Thomas (2002).

The robust measuring techniques yield ambiguous results for the communal roughness parameters, since, from visual inspection, the non-coated surface is smoother than

Table 1: Roughness amplitude spacing parameters for all test surfaces obtained using stylus instrument. Standard deviations based on five samples for each surface are up to approximately 6%.

Param. [μm]	Reference	FR	SPC	Epoxy
R_a	0.193	0.140	1.16	2.05
R_z	1.54	0.935	6.47	9.21
$R_{z,max}$	3.59	2.37	8.83	14.9
R_{Sm}	30.3	66.5	112	388

the FR coated one. The values provide only an idea about the size of the roughness elements for each coating.

Experimental procedure

State of the art electronics, computer-controlled hot-wire calibrator and a LabVIEW software program allowed for straightforward data acquisition during CTA measurements on the four plate surfaces. Two $5\ \mu\text{m}$ Dantec Dynamics hot-wire probes were used during the experiments: one straight-general purpose type (55P11) to measure the instantaneous freestream velocity, and one boundary layer type (55P15) allowing for streamwise velocity measurements within the boundary layer¹. The use of two hot-wire probes allowed for real-time normalization of the boundary layer velocity, resulting in less post-processing as well as correcting measurements for minor fluctuations within the uniform flow field. The system is designed without drift in voltage over time as explained by White & Ergin (2004). Due to the nature of the study, measurements were conducted for turbulent boundary layers only, even though the experimental setup can acquire both laminar and turbulent boundary layers (Ergin, 2016). Calibrations of the hot-wires were performed at a constant temperature. By the used of an automatic air calibrator uncertainties with respect to velocity, direction and temperature were reduced. The relationship between the voltage and the velocity can be approximated by a fifth order polynomial, allowing for linearisation and accurate determination of the velocity when voltage is recorded. Further, temperature corrections were performed for the calibration to be valid. This was done according to Ergin (2016) prior to the linearisation. The temperature correction ensures valid outputs across a larger range of temperatures, given that an increase in temperature of 1 K induces a 2% divergence in velocity.

Velocity profile measurements were conducted for five measurement planes at distances $x = 100\text{mm}$, 200mm , 300mm , 400mm and 500mm from the leading edge for each of the four plate surfaces, corresponding to Re_x ranging from 1.91×10^5 to 9.54×10^5 when conducted at $U_0 = 30\text{m/s}$. Profiles are obtained for 41 points along the z -axis (cross-stream) in the interval from -50mm to 50mm at each measurement plane. Measurement planes and corresponding coordinate system are illustrated in Figure 1. A linear extrapolation of the last measurements to zero is conducted, thus locating the wall at the given point. The amount of steps in the z -direction is required to allow for precise estimates of the wall location using a quadratic fit to all data points. During post-processing the fitted wall locations are subtracted from the wall distances of the measured velocity profiles. The output is given as normalised velocity profiles with $y = 0$ at the wall for each of the 41 measurement points in the cross-stream direction.

RESULTS AND DISCUSSION

The results are presented as time-averaged steady flow fields for each of the coated plates. One boundary layer profile for each Reynolds number is obtained through ensemble averaging of velocity profiles in cross-stream direction on the plates yielding less data to be processed and a more general result. The obtained profiles for the raw data is plotted in Figure 2.

¹Confer Dantec Dynamics (2014) for information on the 55P11 and 55P15 hot-wire probes.

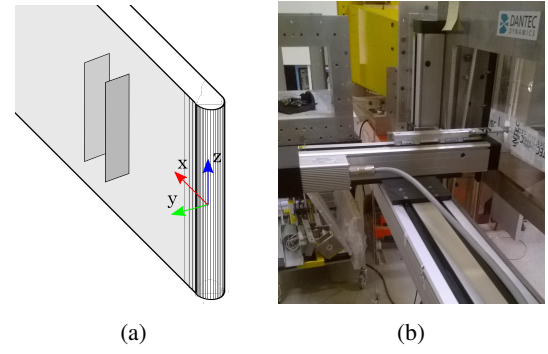


Figure 1: Illustration of two out of five measurement planes (a) with coordinate system for experimental procedure, and experimental setup (b) showing wind tunnel wall, support arm, and traversing system.

To determine skin friction drag coefficients the friction velocity u_τ must be estimated for the given data. Finding u_τ in boundary layers is always a difficult task with no easy way of determining it from direct measurements. A series of indirect methods exist for this purpose, often by assuming some sort of known dependency within the logarithmic layer. This makes it difficult to make any conclusive statements about the logarithmic region for boundary layers that do not follow these tendencies. In the current study, the wall shear stress is determined by fitting the van Driest velocity profile (2) to the obtained boundary layer velocity profiles as suggested by van Driest (1956). The van Driest profile merges the linear profile within the viscous sublayer with the logarithmic profile in the logarithmic region, thus a better estimate of the friction velocity is obtained compared to only considering the logarithmic layer.

The coordinate displacement Δy , approximated by (1) according to Cebeci & Chang (1978), is needed when solving for u_τ and k_s^+ .

$$\Delta y^+ = 0.9 \left[\sqrt{k_s^+} - k_s^+ \exp\left(-\frac{k_s^+}{6}\right) \right]. \quad (1)$$

(1) is valid for $5 < k_s^+ < 2000$, thus applicable to transi-

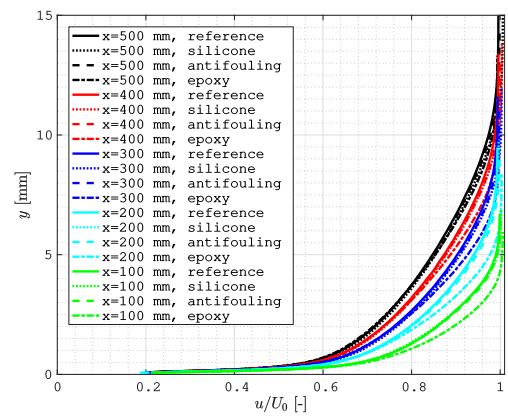


Figure 2: Comparison of ensemble averaged boundary layer velocity profiles at five different measurement planes for all plate surfaces. Obtained from experiments conducted at 30 m/s.

tional and rough wall flows. Using a numerical nonlinear least-squares method, (2) is fitted to each of the profiles in Figure 2 in a non-dimensionalised domain, $u^+ = \frac{\bar{u}}{u_\tau}$ and

$$\bar{u} = 2u_\tau \int_0^{y^+} \frac{1}{1 + \left\{ 1 + 4\kappa^2 (y^+ + \Delta y^2)^2 \left[1 - \exp\left(-\frac{y^+ + \Delta y^+}{A_d}\right) \right]^2 \right\}^{1/2}} dy^+ \quad (2)$$

Table 2: Friction velocities, u_τ [m/s], and roughness Reynolds numbers, k_s^+ [-], obtained from van Driest fitting to each of the velocity profiles. Reynolds numbers are in the order of 10^5 .

Re_x	Reference	FR	SPC	Epoxy	
1.91	k_s^+	12.3	13.2	15.7	21.4
	u_τ	1.62	1.68	1.74	1.90
3.82	k_s^+	11.8	12.3	14.4	18.9
	u_τ	1.56	1.57	1.60	1.68
5.72	k_s^+	11.4	11.8	13.7	17.7
	u_τ	1.50	1.50	1.53	1.58
7.63	k_s^+	11.1	11.4	13.3	17.1
	u_τ	1.47	1.46	1.48	1.52
9.54	k_s^+	10.9	11.2	13.3	16.7
	u_τ	1.44	1.42	1.45	1.48

The determined values for the friction velocities and the roughness Reynolds numbers are given in Table 2. From the values it is apparent that neither of the surfaces give rise to a fully rough flow. Concurrently the reference plate appears not to result in hydraulically smooth flow with k_s^+ ranging between 10.9 and 12.3. Nonetheless, a communal comparison of k_s^+ yields proper results compared to visual inspection, thus supporting the method.

The friction velocities are used to non-dimensionalise the velocity profiles. Figures 3 through 6 depict the effects of Reynolds number as well as roughness on the boundary layer velocities. From Figures 3 and 4 it is clear that there is a tendency for the velocity profiles to collapse onto the same logarithmic layer profile for the same surface roughness, as one would expect (Schultz, 2004). This is the case for Reynolds numbers above $Re_x > 1.91 \times 10^5$ further downstream of the leading edge. At the measurement point closest to the leading edge a deviation from this tendency is observed. The method of fitting requires the presence of a significant logarithmic layer to yield proper results. For the case of lower Reynolds numbers the logarithmic layer is fairly thin, inducing uncertainties to the method of skin friction estimation. Figure 3 shows the fit of the van Driest profile to constant stress layer of the measured velocity data, thus $y < (0.2 - 0.3)\delta$ (van Driest, 1956), with $u(\delta) = 0.99U_0$. When comparing the velocity profiles for each of the coatings at the same Reynolds number in a (u^+, y^+) -domain (confer Figures 5 and 6) a downward shift of the size of the roughness function Δu^+ for increased k_s^+ is observed in accordance with the work of Coles (1956). The

$y^+ = \frac{yu_\tau}{\nu}$ (Schlichting, 1979), using the wall parameters u_τ and ν .

largest Δu^+ is obtained for the epoxy coating. A (u^+, y^+) -plot for $Re_x = 9.54 \times 10^5$ is given in Figure 6. No significant difference in profiles for the coated plates is observed, thus roughness effects appear less significant at higher Reynolds numbers further downstream of the leading edge.

From u_τ the skin friction coefficients are readily calculated for each of the coatings across the range of Reynolds numbers. These are given in Figure 7 as a function of the Reynolds number Re_x . Skin friction coefficients range between $C_f = 8.03 \times 10^{-3}$ and $C_f = 4.45 \times 10^{-3}$, depending on type of coating and distance from measuring point to leading edge. It is interesting to notice that even though the roughness Reynolds numbers are estimated to be higher for the FR coating than the non-coated plate, little difference can be observed between their respective C_f curves. On the other hand, the hot-wire anemometry method combined with the van Driest fitting allows for a clear differentiation between surface where the difference in roughness is slightly higher, e.g. epoxy vs. reference. For comparison and benchmarking of the results the Prandtl-Schlichting interpolation formula for a flat, hydraulically smooth plate at zero angle of incidence as described by Schlichting (1979) is applied. The relation is often used in unison with the ITTC Performance Prediction Method, thus employed here (Chambers *et al.*, 1978). Prandtl-Schlichting's relation agrees quite well with the data, except for $Re_x \leq 3.82 \times 10^5$, probably because the log law applies only over a very lim-

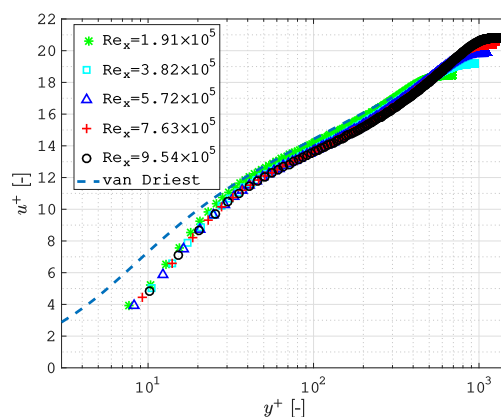


Figure 3: Effect of Reynolds number on mean boundary layer velocity profiles u^+ with respect to y^+ for non-coated plate. Plotted with a semilogarithmic x -axis. The van Driest profile is plotted for the case of $Re_x = 1.91 \times 10^5$ from the obtained values in Table 2.

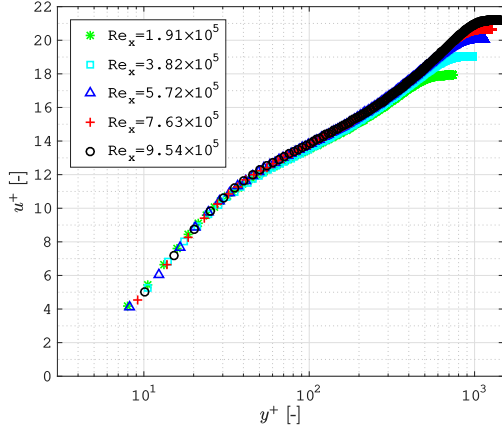


Figure 4: Effect of Reynolds number on mean boundary layer velocity profiles u^+ with respect to y^+ for FR coated plate. Plotted with a semilogarithmic x-axis.

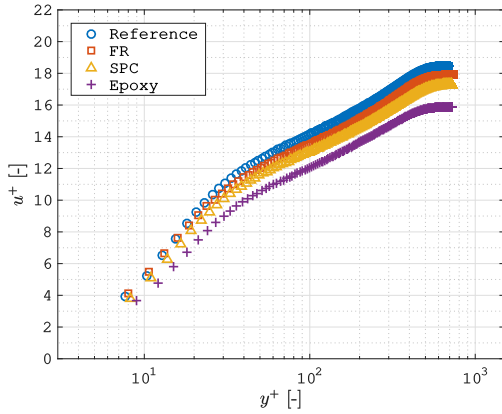


Figure 5: Comparison of mean boundary layer velocity profiles u^+ with respect to y^+ for $Re_x = 1.91 \times 10^5$ in a semilogarithmic plot. Data for each coating is shown.

ited range of wall distances at lower Reynolds numbers. The fact that the empirical relation is consistent with the data provides an interesting result in relation to the experimental setup, since the reference plate is not hydraulically smooth. Later numerical investigations proved that the geometry of the leading edge of the plates caused boundary layer separation in the vicinity of the leading edge, slightly contaminating the results for the 'zero-incidence' skin friction coefficients (Zafiryadis, 2016). Additional sources of error arising from calibrations, temperature variations, accuracy of probe positioning, variations in freestream velocity in wind tunnel, and minor coatings flaws contribute to the overall uncertainty of approximately 2.5% for each velocity profile. Errorbars are plotted for each of the measurement points for the reference plate in Figure 7 for representation. Due to the mentioned drawback of the method for estimating C_f , the uncertainty estimate is increased for $Re_x = 1.91 \times 10^5$.

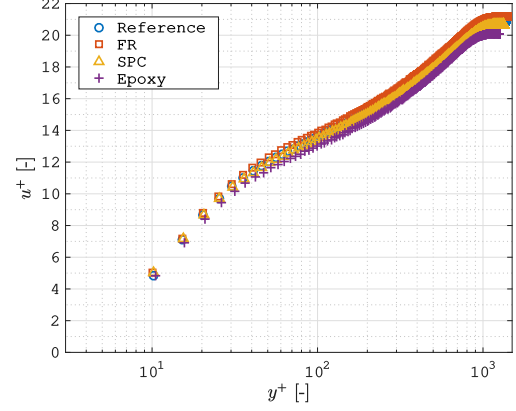


Figure 6: Comparison of mean boundary layer velocity profiles u^+ with respect to y^+ for $Re_x = 9.54 \times 10^5$ in a semilogarithmic plot. Data for each coating is shown.

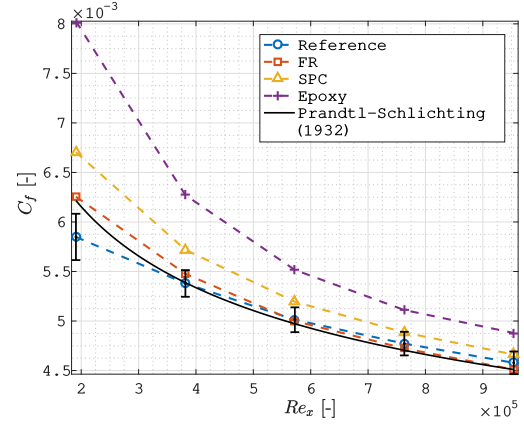


Figure 7: Skin friction coefficients as a function of Reynolds number for all plates. Obtained by fitting of the van Driest velocity profile. Errorbars estimating uncertainty to 2.5%, and 4.0% for lower Re_x , have been added for the reference plate.

Conclusions

Constant temperature anemometry hot-wire measurements were conducted in a wind-tunnel at the Technical University of Denmark to obtain better estimates for skin friction drag coefficients produced by distributed surface roughness of pristine marine antifouling coatings. Boundary layer velocity profiles were obtained for three types of marine coatings (foul release (FR), self-polishing copolymer (SPC), and epoxy coating) applied to aluminium plates with a rounded leading edge. One plate was left uncoated for reference. Measurements spanned a Reynolds number of $Re_x = 1.91 \times 10^5$ to $Re_x = 9.54 \times 10^5$ allowing for estimation of roughness Reynolds numbers k_s^+ and skin friction drag coefficients C_f for each of the coatings as a function of Re_x by fitting with the van Driest velocity profile. The obtained skin friction drag coefficients were found to agree well with the Prandtl-Schlichting formula for the uncoated reference plate as well as the slightly rougher FR coated plate. The highest skin friction coefficients were obtained for the epoxy coated plate. Uncertainties with respect to C_f were estimated to approximately 2.5%, yielding satisfying

repeatability of the data with the possibility of distinguishing the velocity profiles and skin friction coefficients for rough surfaces. Despite attempts to reach adequately high Reynolds numbers, an incomplete similarity was realised with k_s^+ outside of the fully rough regime in which marine coatings operate in full-scale. Thus, extrapolation was deemed idle due to unreal thickness-to-roughness height ratios compared to a full-scale case. Nonetheless, knowledge of the impact of roughness on fluid flow is obtained without information of the characteristics of the surface roughness, a task which is unobtainable using other experimental methods as well as numerical approaches. The technique yielded applicable and accurate C_f predictions for lower Re_x , thus providing a solid foundation for further work on expanding the measurement setup to acquire higher Reynolds numbers suitable for full-scale skin friction drag predictions of pristine and even biofouled antifouling coatings.

Acknowledgements

In addition to the contributions made by the Technical University of Denmark and Dantec Dynamics A/S in terms of financial support and measuring equipment, the close cooperation with Hempel A/S throughout the duration of the study is gratefully acknowledged.

REFERENCES

- Benson, J. 2005 "Boundary-layer response to a change in surface roughness". The University of Reading, Department of Meteorology.
- Bixler, G. D. and Bhushan, B. 2013 "Fluid Drag Reduction with Shark-Skin Riblet Inspired Microstructured Surfaces". *Advanced Functional Materials*, **23**, 2013.
- Candries, M., Atlar, M., Guerrero, A., and Anderson, C.D. 2001 "Lower Frictional Resistance Characteristics of Foul Release Systems". *The 8th International Symposium on practical Design of Ships and other Floating Structures*.
- Cebeci, T and Chang, K.C. (1978) "Calculation of incompressible rough-wall boundary-layer flows". *AIAA Journal* **16**, p. 730.
- Chambers, L. D., Stokes, K. R., Walsh, F. C., and Wood, R.J. 1978 "ITTC Performance Prediction Method". ITTC - Recommended Procedures. Effective date 1999.
- Claire, H. and Yebra, D. 2009 "Advances in marine antifouling coatings and technologies". Woodhead Publishing Limited, 1. edition, pp. 61–67.
- Coles, D. 1956 "The law of the wake in the turbulent boundary layer". Guggenheim Aeronautical Laboratory, California Institute of Technology, Pasadena.
- Dantec Dynamics 2014 "Probes for Hot-wire Anemometry", www.dantecdynamics.com, Publication No.: 238v11.
- Ergin, F. G. 2016 "Natural EU project: Standardised metrology of nano-structured coatings with low surface energy". WP4 report on the results of the automated boundary layer stability experiments. Personal communication.
- Grigson, C. 1992 "Drag Losses of New Ships caused by Hull Finish". *Journal of Ship Research*, **36**, No. 2, pp. 182–192.
- Monaghan, R. J. 1953 "A Review and Assessment of Various Formulae for Turbulent Skin Friction in Compressible Flow". Technical Note No. Aero. 2182, Aeronautical Research Council, p. 11.
- Schlichting, Dr. H. 1979 "Boundary Layer Theory". McGraw-Hill Book Company. 7th edition pp. 201–204, 641–642.
- Schultz, M. P. 2004 "Frictional Resistance of Antifouling Coating Systems. Department of Naval Architecture and Ocean Engineering". United States Naval Academy, Annapolis. *Journal of Fluids Engineering*, **126**.
- Schultz, M.P., Bendick, J.A., Holm, E.R., and Hertel, W.M. 2010 "Economic impact of biofouling on a naval surface ship". *Biofouling*, **27**, No. 1.
- van Driest, E.R. 1956 "On turbulent flow near a wall". *Journal of the Aeronautical Sciences*, **23**, No. 11, pp. 1007–1011.
- Thomas, T.R. 2002 "Rough Surfaces". Longman Group Limited, ISBN: 0-582-46816-7. pp. 21–25, 72–90.
- Vorburger, T. V., Scire, F. E., and Teague, E. C. 1982 "Surface Roughness Measurements of Circular Disks and Their Correlation with Hydrodynamic Drag". Center for Manufacturing Engineering, National Engineering Laboratory, National Bureau of Standard, Washington.
- White, E. B. and Ergin F. G. 2004 "Using laminar-flow velocity profiles to locate the wall behind roughness elements". *Experiments in Fluid*, **36**, No. 5, pp. 805–812.
- Whitehouse, D. J. 1994 "Handbook of Surface Metrology". IOP Publishing Ltd, ISBN: 0-7503-0039-6. pp. 7–21, 102–114.
- Yigit, K. D., Khorasanchi, M., Turan, O., Incelik, A., and Schultz, M. P. 2014 "A CFD model for the frictional resistance prediction of antifouling coatings". Elsevier, Ocean Engineering.
- Zafiryadis, F. L. 2016 "Frictional resistance prediction of antifouling coatings". B.Sc. thesis, Technical University of Denmark.